position of moving eddies on a wide range of scales. The smallest one is the dissipation length η. In a closed flow, the largest one is equal to the system size L. We emphasize the difference with open flows where eddies escape through the open boundaries and the power consumption has gaussian fluctuations[4]. The effective number of degrees of freedom contributing to the turbulence motion can be estimated as $N = (L/\eta)^3$ (ref. 21). Using Kolmogorov mean-field arguments, N can be related to the Reynolds number through $L/\eta = \mathrm{Re}^{4/3}$ (ref. 1). Hence any system of finite Reynolds number can be considered as containing a finite number of degrees of freedom. Given that many scales are important, the simplest scenario is a self-similar one. Indeed, both Kolmogorov's original hypothesis about the energy cascade and subsequent corrections to include intermittency effects assume that the energy transfer per unit mass on scale l, ω_l, has a scale-invariant behaviour (for example, $\langle \epsilon_l^p \rangle \propto l^{\pi(p)}$), as confirmed by experiment[1,22]. In a closed turbulent flow, the scale invariance holds up to the system size. The experimental evidence presented here suggests that this is sufficient to provide a complete analogy with the critical magnetic system and the same kind of universality for $Q_P(P)$ as for $Q_M(M)$.

A consequence of this interpretation is that the fluctuations in the dissipated power can be thought of as a finite-size correction to the result at infinite Reynolds number. The $\mathrm{Re} = \infty$ case is by definition inaccessible for any experiment studying turbulence in a closed flow, as there is a well defined upper and lower length scale between which fluctuations are important. For very small values of Re, one might expect to observe transient effects that depend on the details and dimensions of the experiment, but once some threshold has been exceeded, $Q_P(P)$ should be independent of Re, however large it may be.

As many length scales are important at a critical point, the microscopic details often get washed away and the critical behaviour of apparently radically differing systems can be the same. Only large scale details, such as the symmetry of the hamiltonian and the dimension, are important, and systems with the same critical behaviour are grouped together in 'universality classes'[8]. The probability distribution function for all systems falling in the same universality class should therefore have the same universal form. However, there is no *a priori* reason to expect that the same should be true in going from one universality class to another. It is therefore surprising to find that these two functions are so similar. We do not believe that we have miraculously fallen onto the correct universality class for the turbulent fluid experiment. Rather, it is likely that, for certain universality classes, the departure from gaussian behaviour at a critical point is described to an excellent approximation by the spin-wave limit of the two-dimensional XY model, with the fine details that characterize and separate the universality classes being concentrated in the central part of the distribution function, or otherwise being hidden by experimental errors.

Our results indicate that the universality observed in the turbulence experiment can be explained in terms of a self-similar structure of fluctuations, just as in a finite critical system. This analogy provides an important new experimental application of finite size scaling approaches to a critical point[20] and it suggests a new range of experiments to characterize turbulent flow. Finally, it provides a systematic method of predicting the probability of rare fluctuations in a confined turbulent system. □

Received 26 March; accepted 10 September 1998.

1. Frisch, U. *Turbulence* (Cambridge University Press, Cambridge, 1995).
2. Monin, A. S. & Yaglom, A. M. *Statistical Fluid Mechanics* (MIT Press, Massachusetts, 1975).
3. Eyink, G. L. & Goldenfeld, N. Analogies between scaling in turbulence, field theory and critical phenomena. *Phys. Rev. E* **50,** 4679–4683 (1994).
4. Labbé, R., Pinton, J.-F. & Fauve, S. Power fluctuations in turbulent swirling flows. *J. Phys. II (France)* **6,** 1099–1110 (1996).
5. Zandberg, P. J. & Dijkstra, D. Von Kármán flows. *Annu. Rev. Fluid Mech.* **19,** 465–491 (1987).
6. Archambault, P., Bramwell, S. T. & Holdsworth, P. C. W. Magnetic fluctuations in a finite two-dimensional *XY* model. *J. Phys. A: Math. Gen.* **30,** 8363–8378 (1997).
7. Archambault, P. *et al.* Universal magnetic fluctuations in the 2D-XY model. *J. Appl. Phys.* **83,** 7234–7236 (1998).
8. Wilson, K. G. & Kogut, J. The renormalization group and the ϵ expansion. *J. Phys. Rep. C* **12,** 75–200 (1974).
9. Landau, L. D. & Lifshitz, E. M. *Statistical Physics* Vol. 1 p.9 (Pergamon, Oxford, 1980).
10. Binney, J. J., Dowrick, N. J., Fisher, A. J. & Newman, M. E. J. in *The Theory of Critical Phenomena* 20 (Clarendon, Oxford, 1992).
11. Goldenfeld, N. Lectures on phase transitions and the renormalization group. *Frontiers Phys.* **85,** 279–282 (1992).
12. Kosterlitz, J. M. & Thouless, D. J. Metastability and phase transitions in two-dimensional systems. *J. Phys. C* **6,** 1181–1203 (1973).
13. Berezinskii, V. L. Destruction of long-range order in one-dimensional and two-dimensional systems having a continuous symmetry group *I.* Classical systems. *Sov. Phys. JETP* **32,** 493–500 (1971).
14. José, J. V., Kadanoff, L. P., Kirkpatrick, S. & Nelson, D. R. Renormalization, vortices, and symmetry-breaking perturbations in the two-dimensional planar model. *Phys. Rev. B* **16,** 1217–2141 (1977).
15. Tobochnik, J. & Chester, G. V. Monte Carlo study of the planar spin model. *Phys. Rev. B* **20,** 3761–3769 (1979).
16. Mermin, N. D. & Wagner, H. Absence of ferromagnetism or antiferromagnetism in one or two-dimensional isotropic Heisenberg models. *Phys. Rev. Lett.* **17,** 1133–1136 (1966).
17. Mermin, N. D. Absence of ordering in certain classical systems. *J. Math. Phys.* **8,** 1061–1064 (1967).
18. Bramwell, S. T. & Holdsworth, P. C. W. Magnetization and universal subcritical behaviour in two-dimensional *XY* magnets. *J. Phys. Condens. Matt.* **5,** L53–59 (1993).
19. Binder, K. in *Computational Methods in Field Theory* (eds Gausleven, H. & Lang, C. B.) 59 (Springer, Berlin, 1992).
20. *Finite-Size Scaling, Current Physics Sources and Comments* Vol. 2 (ed. Cardy, J. L.) (North-Holland, 1990).
21. Landau, L. D. & Lifshitz, E. M. *Fluid Mechanics* 123 (Pergamon, Oxford, 1959).
22. Castaing, B., Gagne, Y. & Hopfinger, E. J. Velocity probability density functions of high Reynolds number turbulence. *Physica D* **46,** 177–200 (1990).

Acknowledgements. We thank P. Archambault, S. Fauve, J.-Y. Fortin, R. Labbé and S. Peysson for collaborations leading to refs 4, 6 and 7, and C. Baudet, J. L. Cardy, B. Castaing, M. J. Harris, J. Kurchan and Z. Račz for discussions.

Correspondence and requests for materials should be addressed to P.C.W.H. (e-mail: pcwh@enslapp.ens-lyon.fr).

Observation of 'third sound' in superfluid ^{3}He

A. M. R. Schechter, R. W. Simmonds, R. E. Packard & J. C. Davis

Department of Physics, University of California, Berkeley, California 94720, USA

Waves on the surface of a fluid provide a powerful tool for studying the fluid itself and the surrounding physical environment. For example, the wave speed is determined by the force per unit mass at the surface, and by the depth of the fluid[1]: the decreasing speed of ocean waves as they approach the shore reveals the changing depth of the sea and the strength of gravity. Other examples include propagating waves in neutron-star oceans[2] and on the surface of levitating liquid drops[3]. Although gravity is a common restoring force, others exist, including the electrostatic force which causes a thin liquid film to adhere to a solid. Usually surface waves cannot occur on such thin films because viscosity inhibits their motion. However, in the special case of thin films of superfluid ^{4}He, surface waves do exist and are called 'third sound'. Here we report the detection of similar surface waves in thin films of superfluid ^{3}He. We describe studies of the speed of these waves, the properties of the surface force, and the film's superfluid density.

Superfluid ^{3}He can be described by a 'two fluid' model[4] where the liquid is considered to be two interpenetrating fluids: a normal fluid component and a superfluid component. Each component has a mass density fraction, ρ_n/ρ and ρ_s/ρ respectively, and is governed by a different equation of motion. In particular, the superfluid component flows without viscosity while the normal component experiences viscous drag. This 'two fluid' nature allows several different types of acoustic phenomena to exist. For example, oscillations with both components moving in-phase are called first sound, while out-of-phase oscillations are called second sound.

Third sound[5,6] is the name given to a surface wave travelling on a thin superfluid film. Here, the superfluid component oscillates parallel to the substrate while the normal-fluid component is held stationary by viscosity, as shown schematically in Fig. 1a. A typical wave amplitude is 0.1 nm. In the simplest case, the speed of

a third-sound wave takes the form[5];

$$c_3 = \sqrt{\frac{\langle\rho_s\rangle}{\rho} F\delta} \quad (1)$$

where δ is the film thickness, $\langle\rho_s\rangle$ is the superfluid density averaged over δ, ρ is the density of the liquid, and F is the van der Waals force per unit mass at the film's surface. A possible additional term in equation (1) associated with specific entropy and temperature[7] is negligible for our ^{3}He films.

Third sound has proven to be a powerful probe of fundamental phenomena in superfluid ^{4}He. Examples include measurements of the physics of two-dimensional phase transitions[8], the layered nature of ^{3}He–^{4}He films[9], the non-wetting of alkali metals[10], the generation of vortices and high circulation states[11], and many other phenomena[12–16]. The number and significance of these applications in ^{4}He has stimulated strong interest in whether similar surface waves can exist in films of superfluid ^{3}He[17,18].

Several studies have explored the conditions for superfluidity in films of ^{3}He (refs 19–24), and have shown that it is suppressed when the film thickness is near the characteristic healing length, ξ. This is caused by breaking of p-wave Cooper pairs during scattering from the microscopically rough substrates. Because for ^{3}He $\xi = 65$ nm (at temperature $T = 0$ and zero pressure), we use films with thicknesses near 100 nm.

To search for third sound in ^{3}He we use the apparatus shown schematically in Fig. 1b. The superfluid ^{3}He film resides on the flat top surface of a polished copper disk. The basic experimental idea is to apply oscillating electrical forces to this film thereby exciting standing waves of third sound, and then to detect capacitively the surface motion due to these standing waves.

We performed test experiments in this apparatus[18], using superfluid ^{4}He with films of thickness near 100 nm, which indicated that the perimeter of the substrate reflects the surface waves. Further, the spectrum of ^{4}He third sound is consistent with a 'fixed' boundary condition; that is, the surface displacement is zero near the substrate perimeter. This agrees with several similar experiments, including the first study[6] of third sound in ^{4}He.

For a film of superfluid ^{3}He, solution of the wave equation with fixed boundary conditions at the substrate perimeter indicates that resonant standing-wave modes can exist. These modes are analogous to those in the membrane of a drum head, and their frequencies f are related to the wave speed c_3 by

$$f_{m,n} = c_3 \frac{\alpha_{m,n}}{2\pi R} \quad (2)$$

where the integers m and n are called the mode numbers, R is the radius of the disk, and $\alpha_{m,n}$ is the value of the nth zero of the Bessel function $J_m(x)$; $\alpha_{0,1} = 2.405$, $\alpha_{1,1} = 3.832$, $\alpha_{0,2} = 5.520$, $\alpha_{1,2} = 7.016$, $\alpha_{0,3} = 8.654$ specify the five lowest frequency modes to which this experiment is sensitive. Tests with superfluid ^{4}He in the present cell have identified resonances for these five modes.

In a typical series of superfluid ^{3}He measurements, the cell is cooled below the temperature where the film becomes superfluid, T_c^{film}, with a given film of thickness δ on the substrate. The driving-force frequency is slowly swept from 0.2 Hz to 8 Hz, and the amplitude of the surface response at each frequency is measured at the detector. We repeat this frequency sweep at a range of temperatures. Figure 2a shows the result of a series of such measurements for a film of $\delta = 233$ nm, between 0.32 mK and 0.79 mK. Several resonant modes, whose frequencies vary with changing temperature, are apparent. Similar spectra were acquired at film thicknesses, δ, of 92, 122, 170, 174, 189, 221, 252, 264 and 281 nm. From these, it is clear that well-defined surface-wave modes do exist in superfluid ^{3}He, and that we can identify their resonant frequencies and quality factors. In addition, the frequencies of these modes fall with rising temperature, and the phenomena disappear for $T > T_c^{film}$. These data provide, to our knowledge, the first evidence for the existence of third sound in superfluid ^{3}He.

We can use these third-sound signals to probe the physics of the superfluid ^{3}He films by measuring the wave speed c_3, and by using c_3 to obtain the average superfluid density $\langle\rho_s\rangle/\rho$. First, in order to assign mode numbers to the peaks shown in Fig. 2a, their frequencies are plotted versus temperature (Fig. 2b). We interpret the temperature dependence of the frequencies in terms of the simplest available model, using the following assumptions. First, equations

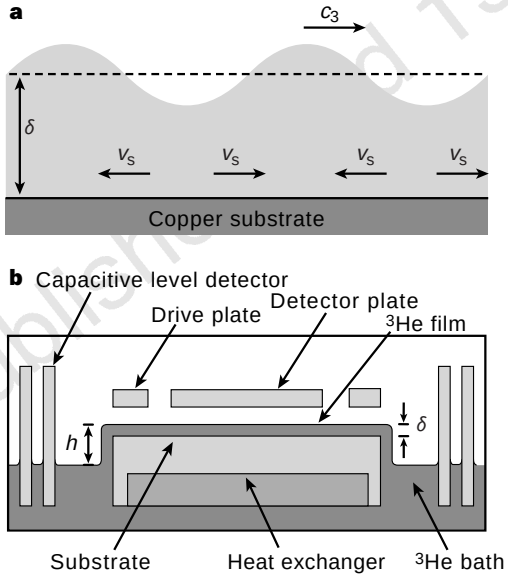

Figure 1 Schematic representations of a third-sound wave and of the experimental apparatus. **a**, The profile of a third-sound wave in which the 'normal-fluid' fraction of the film is kept in place by viscosity and the 'superfluid' fraction oscillates parallel to the substrate, with velocity v_s. This causes local variations in the film thickness while allowing a surface wave to propagate at speed c_3. **b**, A thick horizontal copper disk (radius $R = 19.1$ mm) is positioned in a container of superfluid ^{3}He, its polished top surface forming the substrate for the superfluid film. From a fill line at the bottom of the cell, liquid ^{3}He is introduced to a distance h below the top of the disk. A film of thickness δ forms on the substrate when the temperature falls below the critical temperature for film superfluidity, T_c^{film} (which is less than the bulk superfluid critical temperature $T_c = 0.929$ mK). Two plates are placed above the substrate: a 10.1-mm-radius disk and an annular ring (13.6-mm inner radius and 17.8-mm outer radius). A grounded electrostatic shield (not shown) is positioned between the two electrodes. The geometry of the electrode assembly is designed to minimize the creation of standing waves of third sound on its surfaces. The plates are ~32 μm above the substrate, and are believed to be tilted so that one side is about 20 μm above the other side. This provides sensitivity to azimuthally asymmetric modes on the film. The outer annular electrode is connected to an oscillating voltage of typical amplitude 1 V superimposed on a larger d.c. voltage, typically 10 V. Due to the dielectric constant of the liquid ($\epsilon = 1.0426$) this produces an a.c. driving force on the film's surface. The central disk-shaped electrode is connected to a capacitance bridge that monitors film thickness changes which are occurring synchronously with the a.c. excitation. The system's resolution for average film surface displacement is ~30 pm Hz$^{-1/2}$. A coaxial cylindrical capacitor, mounted vertically, measures the height h from the free surface of the bulk liquid to the substrate. The apparatus is designed for the generation and detection of third sound in films with a range of film thicknesses near 100 nm, in a cell suitable for refrigeration down to $T < 300$ μK. The ^{3}He bath is cooled by a heat exchanger connected to a nuclear demagnetization refrigerator, and its temperature is measured using pulsed NMR on ^{195}Pt. As the substrate itself is isolated from electrical ground, thermal contact from it to the bath is made via a second heat exchanger, installed in the bottom of the substrate before polishing. The substrate was machined with a regular cutting tool and then polished to an apparent mirror finish by lapping. A series of diminishing grit sizes down to 0.25 μm were used.

(1) and (2) are combined to show that the mode frequencies are proportional to $(\langle\rho_s\rangle/\rho)^{1/2}$. Second, using a Landau–Ginzburg model[24] which states that $\langle\rho_s\rangle/\rho \propto (1 - T/T_c^{film})$, we find that the mode frequencies $f_{m,n} \propto (1 - T/T_c^{film})^{1/2}$. We define T_c^{film} to be the measured temperature at which the film's motion in response to applied voltages disappears. The proportionality constant is identified by fitting the predicted frequencies for the third radial mode ($m = 0, n = 3$) to the frequencies of the (0,3) mode in the data. The predicted frequencies for the lower-frequency modes are then determined, and are shown as the solid lines in Fig. 2b.

The observed spectra clearly have features in common with the predictions of this simple model, allowing us to identify the mode numbers for several peaks. But other peaks are not in as good agreement, indicating that the surface waves are revealing new complexities in the physics of the ^{3}He film. For example, as T decreases we observe a behaviour involving the mixing and splitting of several lower-frequency modes, which is so far unexplained. Similar behaviour, both in the general agreement of several modes with the model, and in the unexpected splittings, have been observed for all other measured film thicknesses.

We use the observed frequencies of the (0,3) mode—because this mode is clearly identifiable for all films and temperatures—to determine c_3. We believe that the (0,3) is most reliable because geometrically it has the strongest overlap with the drive capacitor plate. Figure 3a shows the values of c_3 deduced from equation (2) for several film thicknesses, as a function of temperature. These speeds are very low in comparison with ^{4}He, but they lie in the expected range for superfluid ^{3}He. At low temperatures, c_3 at first rises with δ; but, when δ nears 170 nm, the speed begins to fall again. We believe that this behaviour arises from the competition between $\langle\rho_s\rangle$ rising with δ, and the van der Waals force F falling with δ.

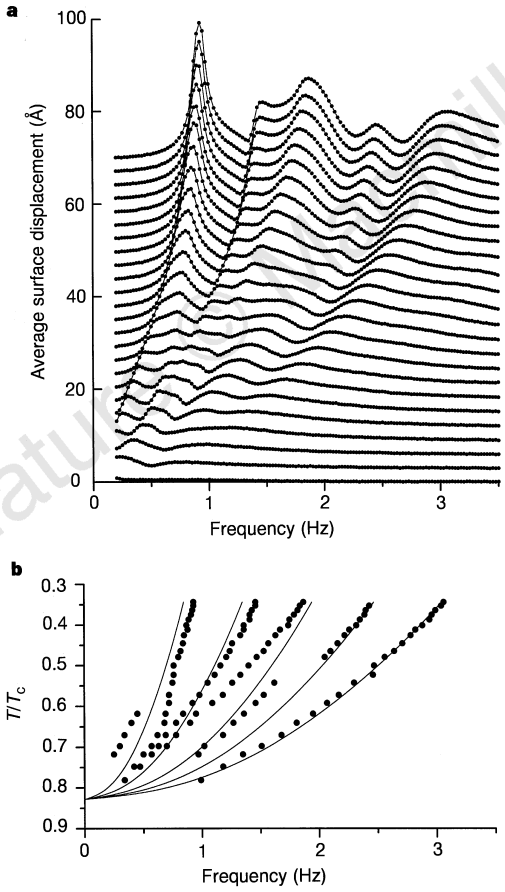

Figure 2 ^{3}He third-sound spectra, and the resonant frequencies as a function of temperature. **a**, A typical series of third-sound spectra for several different temperatures with $\delta = 233$ nm. The temperature ranges from 0.79 mK, just below the onset of superfluidity at T_c^{film} for the lowest curve, to 0.32 mK for the highest curve, with approximately even temperature steps. The curves are shifted vertically from each other for clarity of presentation. Similar spectra were acquired at film thicknesses $\delta = 92, 122, 170, 174, 189, 221, 252, 264$ and 281 nm. **b**, Frequencies of the observed peaks versus T/T_c. The solid lines represent the expected distribution of the peaks from the simple model described in the text.

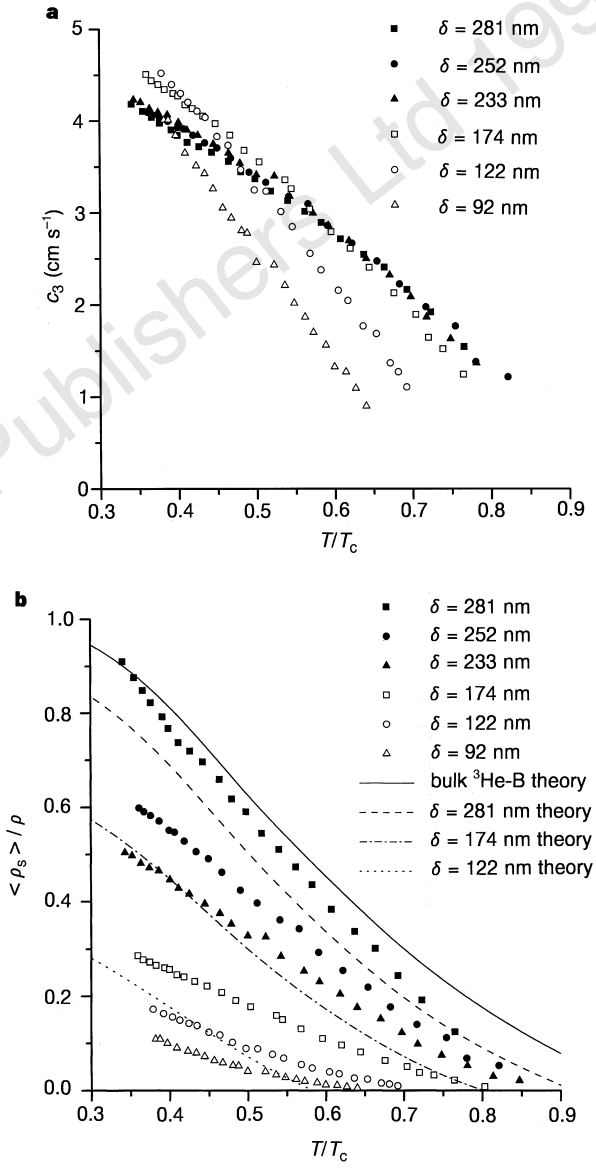

Figure 3 The speed of ^{3}He third sound and the associated superfluid density as a function of temperature. **a**, The speed of third-sound waves deduced from equation (2) for films with $\delta = 92, 122, 174, 233, 252$ and 281 nm, as a function of temperature. We show the value of c_3 as calculated from the frequency of the (0,3) mode using equation (2). The calculated values for c_3 using the frequencies of the other modes are in reasonable agreement with the data shown. The standard deviation for c_3 of any particular δ and T has a maximum value of 12%. For clarity, data is shown from only a subset of the measured films, but the speeds calculated for all the other films are also in good agreement with those shown. **b**, The average superfluid density of the film obtained from the speed of third sound and equation (1), as a function of temperature for films with $\delta = 92, 122, 174, 233, 252$ and 281 nm. The dashed lines represent the prediction of a model for a thin ^{3}He-B film with diffusive scattering of the Cooper pairs from the substrate and specular scattering from the surface of the film for three film thicknesses $\delta = 122, 174$ and 281 nm. The solid line is the bulk superfluid density of ^{3}He at zero pressure.

The superfluid fraction $\langle\rho_s\rangle/\rho$, contains fundamental information on the wave speed, the thermodynamics of the superfluid film, and the effects of disorder. To find $\langle\rho_s\rangle/\rho$ from equation (1), we need to know both δ and the van der Waals force F.

The value of F can be determined because the van der Waals potential $U(\delta)$ and the gravitational potential are equal at the surface of the film, that is

$$U(\delta) = gh(\delta) \quad (3)$$

where $h(\delta)$ is the height of the film above the bulk surface, and g is the acceleration due to gravity. This equilibrium occurs because the entire free surface of a superfluid is at a constant chemical potential[25]. The film thickness is varied by introducing additional ^{3}He to reduce h. We find $U(\delta)$ by determining δ for various heights h, and fitting a smooth curve to our data for $h(\delta)$. Finally, we calculate the force from $F = -\mathrm{d}U/\mathrm{d}\delta = -g\mathrm{d}h/\mathrm{d}\delta$.

We determine δ from the capacitance between the substrate and the electrode above it. On the basis of comparison between $\delta(h)$ measurements in ^{3}He, and those in ^{4}He where both surfaces are covered, it seems that films of equal thickness reside on both electrodes. We assume that the electrodes are smooth and flat. Our measured $h(\delta)$ for ^{3}He can be expressed as $h = (\alpha/\delta)^n$ where $\alpha = (10.0 \pm 0.4) \times 10^{-9}$ (in units of metres$^{4/3}$) and $n = 3$. This is in reasonable agreement with previous measurements[20] which found $\alpha = (12.0 \pm 0.5) \times 10^{-9}$ metres$^{4/3}$ and $n = 3$. The height h is measured using an annular capacitor which varies linearly with liquid height.

Substituting the measured values of δ, $F(\delta)$ and c_3 into equation (1), we find the values of $\langle\rho_s\rangle/\rho$ for the same films as in Fig. 3a. The results (Fig. 3b) indicate that as the films are made thicker, T_c^{film} rises (approaching the bulk value T_c). Also, for any given temperature, $\langle\rho_s\rangle/\rho$ rises with increasing film thickness. These observations are as expected when disorder in the substrate surface causes breaking of the ^{3}He Cooper pairs[22]. Suppression of superfluidity also occurs in the presence of strong disorder within the bulk liquid, for example, ^{3}He in aerogel[26]. The dashed lines shown in Fig. 3b are theoretical predictions[27] for the $\langle\rho_s\rangle/\rho$ of thin superfluid ^{3}He-B films in the presence of disorder, and are in reasonable agreement with observations for our thickest films.

The quality of agreement between theory and observation for both the spectrum and $\langle\rho_s\rangle/\rho$, especially for the thickest films, is further evidence that the ^{3}He third sound is governed by equation (1). However, several unexpected observations have also been made with this probe. For films where $\delta < 3\xi$, $\langle\rho_s\rangle/\rho$ departs significantly from predictions and may indicate a change to an A-like phase, or the approach of true two-dimensionality in this superfluid[28]. The complexity of the spectral features may also reflect unanticipated properties of this system. Although an isotropic superfluid film like ^{4}He should have no mixing of modes, ^{3}He is an anisotropic superfluid in which several sources of coupling might be possible, including textural effects, and a Hall effect phenomenon[29] due to the ordering of the angular momentum of the Cooper pairs in the A-phase. These issues will be addressed in future work.

The observation of third sound in superfluid ^{3}He opens the door to the study of a number of important phenomena for which, until now, no experimental technique was available. These include the limit on how thin a ^{3}He film can be made and still remain superfluid, the transition to two-dimensional superfluidity possibly via a Kosterlitz–Thouless vortex unbinding phase transition[28], the superfluid analogue of the quantum Hall effect[29], and the potential for two-dimensional ^{3}He superfluidity in submonolayer coverages via a new mechanism[30]. □

Received 1 July; accepted 29 September 1998.

1. Landau, L. D. & Lifshitz, E. M. *Fluid Mechanics* 36–44 (Pergamon, Oxford, 1959).
2. Bildsten, L. & Cutler, C. Nonradial oscillations in neutron star oceans: a source of quasi-periodic x-ray oscillations? *Astrophys. J.* **449,** 800–812 (1995).
3. Whitaker, D. L., Weilart, M. A., Vincente, C. L., Maris, H. J. & Seidel, G. M. Oscillations of charged helium II drops. *J. Low Temp. Phys.* **110,** 173–178 (1998).
4. Tilley, D. R. & Tilley, J. *Superfluidity and Superconductivity* 77–83 (Hilger, Bristol, 1986).
5. Atkins, K. R. Third and fourth sound in liquid helium II. *Phys. Rev.* **113,** 962–965 (1959).
6. Everitt, C. W. F., Atkins, K. R. & Denenstein, A. Third sound in liquid helium films. *Phys. Rev.* **136,** A1494–A1499 (1964).
7. Bergman, D. Hydrodynamics and third sound in thin HeII films. *Phys. Rev.* **188,** 370–384 (1969).
8. Rudnick, I. Critical surface density of the superfluid component in ^{4}He films. *Phys. Rev. Lett.* **40,** 1454–1455 (1978).
9. Ellis, F. M., Hallock, R. B., Miller, M. D. & Guyer, R. A. Phase separation in films of ^{3}He-^{4}He mixtures. *Phys. Rev. Lett.* **46,** 1461–1464 (1981).
10. Ketola, K. S., Wang, S. & Hallock, R. B. Anomalous wetting of helium on cesium. *Phys. Rev. Lett.* **68,** 201–204 (1992).
11. Ellis, F. M. & Li, L. Quantum swirling of superfluid helium films. *Phys. Rev. Lett.* **71,** 1577–1580 (1993).
12. Sheldon, P. A. & Hallock, R. B. Third sound and energetics in ^{3}He-^{4}He mixture films. *Phys. Rev. B* **50,** 16082–16085 (1994).
13. Brisson, J. G., Mester, J. C. & Silvera, I. F. Third sound of helium on a hydrogen substrate. *Phys. Rev. B* **44,** 12453–12462 (1991).
14. Ekholm, D. T. & Hallock, R. B. Studies of the decay of persistent currents in unsaturated films of superfluid ^{4}He. *Phys. Rev. B* **21,** 3902–3912 (1980).
15. Pickar, K. A. & Atkins, K. R. Critical velocity of a superflowing liquid-helium film using third sound. *Phys. Rev.* **178,** 389–399 (1969).
16. Cho, H. & Williams, G. A. Vortex core size in submonolayer superfluid ^{4}He films. *Phys. Rev. Lett.* **75,** 1562–1565 (1995).
17. Eggenkamp, M. E. W. *et al*. On the possibility of observing third sound on ^{3}He. *J. Low Temp. Phys.* **110,** 299–304 (1998).
18. Schechter, A. M. R., Simmonds, R. W. & Davis, J. C. Capacitive generation and detection of third sound resonances in saturated superfluid ^{4}He films. *J. Low Temp. Phys.* **110,** 603–608 (1998).
19. Sachrajda, A., Harris-Lowe, R. F., Harrison, J. P., Turkington, R. R. & Daunt, J. G. ^{3}He film flow: two-dimensional superfluidity. *Phys. Rev. Lett.* **55,** 1602–1605 (1985).
20. Daunt, J. G. *et al*. Critical temperature and critical current of thin-film superfluid ^{3}He. *J. Low Temp. Phys.* **70,** 547–568 (1988).
21. Davis, J. C., Amar, A., Pekola, J. P. & Packard, R. E. Superfluidity of ^{3}He films. *Phys. Rev. Lett.* **60,** 302–304 (1988).
22. Xu, J. & Crooker, B. C. Very thin films of ^{3}He: a new phase? *Phys. Rev. Lett.* **65,** 3005–3008 (1990).
23. Freeman, M. R., Germain, R. S., Thuneberg, E. V. & Richardson, R. C. Size effects in thin films of superfluid ^{3}He. *Phys. Rev. Lett.* **60,** 596–599 (1988).
24. Jacobsen, K. W. & Smith, H. Critical current for the flow of superfluid ^{3}He in a confined geometry. *J. Low Temp. Phys.* **67,** 83–89 (1987).
25. Tilley, D. R. & Tilley, J. *Superfluidity and Superconductivity* 92–94 (Hilger, Bristol, 1986).
26. Porto, J. V. & Parpia, J. M. Superfluid ^{3}He in aerogel. *Phys. Rev. Lett.* **74,** 4667–4670 (1995).
27. Freeman, M. R. *Size Effects in ^{3}He Films.* Thesis, Cornell Univ. (1988).
28. Stein, D. L. & Cross, M. C. Phase transitions in two dimensional superfluid ^{3}He. *Phys. Rev. Lett.* **42,** 504–507 (1979).
29. Volovik, G. E. An analog of the quantum Hall Effect in a superfluid ^{3}He film. *Sov. Phys. JETP* **67,** 1804–1811 (1988).
30. Kurihara, S. Singlet superfluidity in ^{3}He film on ^{4}He film. *J. Phys. Soc. Jpn* **52,** 1311–1316 (1983).

Acknowledgements. We thank L. Bildsten, R. B. Hallock, D.-H. Lee, J. M. Goodkind, O. Ishikawa, J. Harrison and G. Williams for discussions. This work was supported by the NSF, the ONR and by the Packard Foundation.

Correspondence and requests for information should be addressed to J.C.D. (e-mail: jcdavis@socrates.berkeley.edu); see also http://socrates.berkeley.edu/~davisgrp.

Monochromatic electron emission from the macroscopic quantum state of a superconductor

K. Nagaoka*, T. Yamashita*, S. Uchiyama*, M. Yamada*, H. Fujii* & C. Oshima*†

** Department of Applied Physics, Waseda University, 3-4-1, Okubo, Shinjyuku-ku, Tokyo 169-8555, Japan*
† Kagami Memorial Laboratory for Material Science and Technologies, Waseda University, 2-8-26, Nishiwaseda, Shinjyuku, Tokyo 169-0051, Japan

The ground state of a superconductor is a macroscopic quantum state that can extend coherently over substantial distances[1]. As a result, electrons tunnelling from two different points (separated by macroscopic length) on the surface of a superconductor remain coherent in phase and so are able to interfere: this property forms the basis of superconducting quantum interference devices (SQUIDs). Another characteristic of electrons tunnelling from a superconductor is that they are monochromatic, their energy being determined by the ground-state energy of the superconducting state. Monochromatic electrons have been observed